U.S. DEPARTMENT OF COMMERCE
NATIONAL OCEANIC AND ATMOSPHERIC ADMINISTRATION
NATIONAL WEATHER SERVICE
NATIONAL METEOROLOGICAL CENTER

OFFICE NOTE 206

Axi-Symmetric Analysis of the Hurricane Vortex with the Aid of Two-Dimensional Model Statistics

Robert E. Livezey
Development Division

AUGUST 1979

Axi-Symmetric Analysis of the Hurricane Vortex with the Aid of Two-Dimensional Model Statistics

Robert E. Livezey

ABSTRACT

At the National Meteorological Center an effort is underway to blend and assimilate reconnaissance and satellite data into an axial-symmetric hurricane model (used for 3-D model initialization). The method consists of the assignment of a target rotational wind field for use in a dynamic-initialization step. The assignment uses limited real data and a statistical history of the model's response to forcing, and is patterned after optimum interpolation. Cross-covariance fields of model solutions are used as influence functions, for data-quality control, and for specification of minimum data requirements.

CONTENTS

1. Introduction

During the 1977 and 1978 hurricane seasons a small number of vortex penetration reconnaissance flights successfully demonstrated that high-accuracy vortex-scale data can be delivered in real time to Weather Service users via the ASDL (Aircraft-Satellite Data Link) system. Encouraged by these tests, both NOAA and USAF are giving serious consideration to the conversion of the entire reconnaissance fleet to this system.

At NMC a first attempt to exploit this data set has consisted of determination of the symmetric part of the storm at one level and its dynamic assimilation in the two-dimensional axi-symmetric model used by the MFM (Movable-area Fine-mesh Model) for vortex initialization. The importance of proper treatment of the symmetric component had been suggested by recent experiments (e.g., Deaven, 1979).

The technique of nudging (Hoke, 1976), in which the model is forced towards data through use of artificial diffusion terms in the tendency equations, was the choice for the dynamic assimilation step. It, however, is usually unsuccessful unless performed at every grid point on a model domain. As a result, it was necessary to devise a technique whereby a few pieces of data could be spread in a physically-meaningful and model-compatible way over the entire axi-symmetric grid. The method also had to be flexible enough to handle different data types and accuracies. This note[1] is a description of the analysis approach finally adopted. A second note will detail the preparatory processing, including extraction of the axi-symmetric component of the ASDL data, while a discussion of the nudging process will appear elsewhere.[2]

2. Theory

The analysis procedure is basically that of optimum interpolation (Gandin, 1963). Features unique to this application are the manner in which correlation fields are specified and the way consistency checks are carried out.

Using Bergman's (1978) notation a variable can be decomposed as

$$F = \overline{F} + f,$$

where the overbar denotes an ensemble mean and f is the deviation of F from this mean. Given n pieces of data, a scaled estimate of the variable,

---

[1]A substantial portion of the material herein was presented at the AMS Twelfth Conference on Hurricanes and Tropical Meteorology, New Orleans, La., April 24-27, 1979.

[2]Postprints, AMS Fourth Conference on Numerical Weather Prediction, Silver Spring, Md., October 29-November 1, 1979.

denoted by the hat, at a given point "a" is then given by

$$\hat{f}_a/(\overline{f_a^2})^{\frac{1}{2}} = \sum_{i=1}^{n} c_i'(f_i + \varepsilon_i)/(\overline{f_i^2})^{\frac{1}{2}},$$

where the subscript i refers to a piece of data, c_i' its weight, and ε_i its error.

The weights are given in optimum interpolation by solution of the linear system

$$\sum_{j=1}^{n} (\mu_{ij} + \delta_{ij}\sigma_j^2)c_j' = \mu_{ai}, \quad i = 1,\ldots,n,$$

$$\mu_{ij} \equiv \overline{f_i f_j}/(\overline{f_i^2}\,\overline{f_j^2})^{\frac{1}{2}}, \qquad (1)$$

$$\sigma_j \equiv (\overline{\varepsilon_j^2}/\overline{f_j^2})^{\frac{1}{2}}.$$

Here, spatial correlations of errors and error-data correlations have been neglected.

With suitable ensemble statistics available, Eqns. (1) can be used to perform analyses on the 20x10 radial-sigma grid of the so-called "spin-up" model. The data matrix (in parentheses on the left-hand side) is Hermitian and positive-definite and after conditioning can be rapidly factorized. Once this is done the system can be solved quickly and accurately at each grid point by recursion. A more efficient approach suggested by Ghil et al. (1979) is not needed here because of the relatively small number of data and/or grid points, but may prove useful in more complex applications.

The principal difficulty in applying these ideas to the hurricane is the specification of the μ- and σ-fields. Existing data bases are inadequate to provide these correlation fields, and modeled correlation forms only take into account scale and local physical relationships (like the geostrophic wind). These latter deficiencies are especially damaging in applications (like the current one) where recurring structural features that exist outside data-rich areas and whose variations are large (like the outflow anticyclone) need to be represented.

On the other hand, auto- and cross-correlations derived from an ensemble of model solutions can retain memory of long-range, strong teleconnections (like cyclone-anticyclone coherence) across the ensemble, as well as subtle but shorter range coherent relationships. Thus, such an ensemble was obtained by integration of the spinup model to 90 hours (to quasi-steadiness) with 92 different sets of operationally-acquired boundary conditions (84 were retained).

Complete correlation fields can then be determined on the model grid and all required statistics in Eqs. (1) can be estimated by bilinear interpolations from the grid. If the spinup model is in fact a realistic representation of

the symmetric part of the hurricane resolvable on the scale of the model (presently 60 km horizontal and 10 layers vertical), its use to develop the correlation fields has some theoretical basis as well as attractive properties. In subsequent sections the practical limitations of these ideas will be explored along with steps that can be taken to ensure proper application of the approach.

3. Model Realism and Data Sources

Because one of the conditions for use of the spinup model in determination of correlation fields is its realism, the tangential wind-field from a typical ensemble member is shown in Fig. 1 to exemplify the model's strengths and weaknesses. Despite the lack of sophisticated treatment of such things as the planetary boundary layer or eddy flux processes, the solution compares favorably to composite storms (e.g., Frank, 1977). The effect of scale is evident to the left of the vertical line where the tangential wind-speed is grossly underestimated and the details of the eye are lost.

It appears that the model can be used as a basis for the analysis with the following caveat: Only data that originate from properly-modeled portions of the storm and that have undergone processing to make it conform to the model geometry and scale should be input to the analysis.

For example, from the figure only tangential wind data from beyond 90 to 150 km should be used and only after azimuthal averaging and smoothing to the 60km scale. This preprocessing is possible with sufficient accuracy for at least ASDL tangential winds and potential temperature, and for the time being these data will provide the principal input to the analysis.

4. Auto- and Cross-Correlation Fields

In general terms, the confidence with which an adjustment can be made of a gridpoint variable from its mean based on a piece of data depends on the absolute value of the cross-correlation between the deviations from ensemble means at the two points. Several sources of data in the hurricane vortex are illustrated schematically in Fig. 1. It is evident that, even if azimuthal averaging and height problems associated with 15-min (or more frequent) picture satellite cloud-tracked winds are solved, the total data supply for this problem will still be extremely small.

Thus, with so few data, a meaningful major adjustment over most of the grid domain can only take place when strong auto- and cross-correlation relationships are widespread. In other words, model variability must be relatively coherent across the ensemble. The autocorrelation field (Fig. 2a) for tangential wind-speed at a midlevel point 210 km from the center suggests that this is the case for at least this variable at this point. All areas shown with $|\mu_{ij}|>.8$ can be confidently adjusted from knowledge of only v_{45}[3], while areas with $|\mu_{ij}|<.8$ will be decreasingly influenced by this datum.

---

[3]Subscripts refer to figure coordinates.

The correlation field for v_{45} derived from a nonrandom subensemble of 25 storms is shown in Fig. 2b to underline the completeness and representativeness of the ensemble. The stable reproduction of the major features of the full ensemble is typical of all studied subensembles with as few as 20 members. While the autocorrelation field is weakened slightly from Fig. 2a to 2b, generally subensemble field strength is maintained and in some cases increased slightly over that of the full ensemble.

Consistent additional data often enhances the ability of the analysis to significantly modify large portions of the model domain. An example is given in Fig. 3 where Fig. 2b is repeated at the top and the corresponding field for a tangential wind in the anti-cyclone is presented at the bottom. The addition of this datum extends the effective range of the analysis by 5-10% of the domain.

5. Subensemble Use

While the ensemble mean storm exemplified in Fig. 2a is well within the overall range of response of the spinup model, it may represent an extreme response for some sets of boundary forcing. This is illustrated schematically in Fig. 4. Thus, it is possible that in some situations an inappropriate target field for nudging could be specified.

This is because in any anticipated application as much as 20-30% of the grid will be modified little from the ensemble mean. When the ASDL data source fails entirely, either from an aborted mission or data rejection by objective techniques described in the next section, the method will return the mean over the entire grid.

Because of the stability of the ensemble statistics, these difficulties can be avoided by use of an appropriate subensemble for specification of the mean and correlation fields in each case. The particular subensemble is selected by a ranking procedure.

Once the storm latitude, sea surface temperature, and lateral sounding are known for a case, a set of characteristics are computed against which stored boundary and forcing characteristics of the entire ensemble are compared and ranked for similarity characteristic by characteristic. Six such measures of similarity are used: Latitude, sea-surface temperature, boundary-layer temperature gradient, boundary-layer moisture gradient, pseudo-equivalent potential temperature lapse in the lateral sounding's 1000-500 mb layer, and the total static energy of the sounding in the same layer.

Individual ranks for each member of the ensemble are combined to form a weighted composite rank (the weights for the list of characteristics above are 1/4, 1/4, 1/8, 1/8, 1/8, 1/8, respectively). The 25 ensemble members with the smallest composite rank then make up the subensemble on which the current analysis is based. In this manner a reasonable target analysis is guaranteed in no-data or limited data situations as long as the input data is internally consistent. This last problem will be addressed next.

6. Absolute Value and Consistency Checks

Despite the condition for use of model statistics given in Section 2 and the caveat for data use in Section 3, inevitably the analysis method will be confronted with inaccurate or inconsistent (with respect to the model ensemble) data. This might occur because of nonrandom errors, incorrect or incomplete data preprocessing to the model reference frame, use of data from improperly modeled storm sectors, or incomplete model statistics.

Whatever the cause, if this data is analyzed the resulting field will be of uncertain validity. For example, the tangential winds and temperatures in Table 1 were produced by an improper estimate of the symmetric part of an ASDL data set and analyzed by the methods outlined above without first being subjected to consistency checks. The result is shown in Fig. 5a and is clearly absurd.

Table 1

Datum	Radius (km)	Sigma
17.52 (m/sec)	150	.9
15.19	210	.9
13.94	270	.9
302.49 (°C)	150	.9
302.03	210	.9
302.16	270	.9

Obviously a check of the reasonableness of a single piece of data can be based on the magnitude of its deviation relative to its standard deviation, i.e., $|f_i|/(\overline{f_i^2})$. To check consistency of any pair of data so-called "structure functions" are formed:

$$s_{ij}^{\pm} = \frac{(f_i+\varepsilon_i)}{(\overline{f_i^2})^{\frac{1}{2}}} \pm \frac{(f_j+\varepsilon_j)}{(\overline{f_j^2})^{\frac{1}{2}}} \quad , \quad \overline{s_{ij}^{\pm}} = 0,$$

$$\rho_{ij}^{\pm} = \sqrt{\overline{s_{ij}^{\pm 2}}} = \sqrt{2(1\pm\mu_{ij}) + \sigma_i^2 + \sigma_j^2} \ .$$

Equations (2) are derived with the assumptions of Section 2.

For any pair of data the ratio $|s_{ij}^{\pm}|/\rho_{ij}^{\pm}$ form the basis for evaluation of consistency of the pair. For positively correlated data the negative test is the severest and vice versa. In other words, the more (less) highly correlated two pieces of data are the more (less) coherent their deviations from the mean are across the ensemble. Weak (strong) positive (negative) correlations imply that a wide (narrow) range of realizations are reasonable for $s^-(s^+)$. These ideas are summarized in plots of Eq. (2) in Fig. 6.

Without consideration of RMS error the checking tools described above are applied to an input data set in the following manner and order:

1. All v's or Θ's are deleted with $|f_i|/(\overline{f_i^2})^{\frac{1}{2}} > 2.0$.
2. The fewest v's are deleted such that all remaining $|s^{\pm}_{v_i v_j}|/\rho^{\pm}_{v_i v_j} \leq 2.0$.
3. All Θ's are deleted that lead to $|s^{\pm}_{v_i \Theta_j}|/\rho^{\pm}_{v_i \Theta_j} > 2.0$.
4. The fewest Θ's are deleted such that all remaining $|s^{\pm}_{\Theta_i \Theta_j}|/\rho^{\pm}_{\Theta_i \Theta_j} \leq 2.0$.

Note that in this procedure, winds are given preference over temperatures.

In Steps 2 and 4, all combinations of candidate data starting with combinations of 1 and progressing upward are checked until successful combinations are found. In the case of a tie (for example 3 different combinations of 2 suffice to clean up the submatrix but no combinations of 1), the combination selected is the one that leaves after elimination the smallest total scaled deviations from the mean.

Application of these steps to the data in Table 1 leads to the deletion of the third wind and first and second temperatures and results in the very reasonable analysis shown in Fig. 5b. More lenient criteria may be just as effective; the major culprits here were the data at 270 km and, with a 3.5 standard deviation cutoff, the first two temperatures would have been retained but the third along with its accompanying wind thrown out. In any case, deviations of both the data and their structure functions provide powerful objective benchmarks for editing and prevention of misapplication of the analysis scheme.

7. Analyzed Fields

A final consideration for the analysis problem here is the selection of which variables to analyze. In Section 3 it was noted that properly preprocessed radial profiles of tangential wind speed and potential temperature seem to be possible for many ASDL missions. Here the feasibility of analyzing these two variables is examined.

Correlation fields for subensemble #54 of v_{45} with both v_{ij} and $_{ij}$ are reproduced in Figs. 7a and 7b, respectively, and give a representative picture of the assignment power of each variable for the rotational wind. Tangential winds from virtually all the low- to mid-troposphere, at all depths near the storm center, and in the vicinity of the anticyclone are useful for analyzing v_{45} and vice versa--the pattern of Fig. 7a is typical of patterns for most v_{ij}'s from the noted regions. In contrast only temperatures in the low- through mid-troposphere near the storm center have much impact on the analysis of v_{45}. This is also true for most v_{ij} in the low- to mid-layers, with rotational wind specification above these levels little affected by temperatures anywhere.

The situation for temperature analysis (illustrated in Fig. 8) is quite different. Temperature autocorrelation plots, exemplified by Fig. 8a, generally have much smaller areas of high coherence than their rotational wind counterparts (Fig. 7a). In fact the high correlation area shown here for Θ_{45} is atypically large compared to most Θ_{ij}-plots. Examination of Fig. 8b, after reversing one's point of view from that of Fig. 7b, reveals that only tangential winds from mid- and low-layers are useful for temperature specification and only near the center of the storm.

Overall, it would take considerably more data to do a temperature analysis comparable in completeness and detail to the wind analysis. Fortunately, nudging theory and experience (Hoke, 1976) suggest that forcing to the rotational wind component at these scales is superior to nudging to the mass field alone or in combination with v and just as effective as nudging to both components of the wind.

8. Further Applications

Alternative uses for the correlation fields and methods described above include increased evaluation capability of both model validity and data suggested by the discussions in Sections 6 and 7, respectively. First, the inability of properly preprocessed data sets of known quality to pass the tests of Section 6 might imply a fundamental model deficiency for a specific regime or subdomain. Second, information on data impact similar to that obtained by Anthes (1974) can be obtained but in considerably more detail and without his case dependency by utilization of combinations of charts like Figs. 7 and 8.

Beyond these applications an attempt is planned to use the two-dimensional correlation fields to guide the design of correlation functions for sparse-data three-dimensional hurricane analysis. More generally, the ideas of developing correlation fields with a numerical model of a structure and application of these fields in analysis after reorientation with respect to the atmospheric analog perhaps ought to be considered in other special problems.

References

Anthes, R. A., 1974: Data assimilation and initialization of hurricane prediction models. J. Atmos. Sci., 31, 702-719.

Bergman, K. H., 1978: Role of observational errors in optimum interpolation analysis. Bull. Am. Meteor. Soc., 59, 1603-1611.

Deaven, D. G., 1979: Movable-area Fine-mesh Model (MFM) performance and research efforts in 1978. Paper presented at 33rd Interdepartmental Hurricane Warning Conference, Jan. 2-4, Homestead AFB, Fla.

Frank, W. M., 1977: The structure and energetics of the tropical cyclone. I. Storm structure. Mon. Wea. Rev., 105, 1119-1135.

Gandin, L. S., 1963: Objective Analysis of Meteorological Fields. Gidrometeorologicheskoe Izdatelstvo (GIMIZ), Leningrad. (English translation, Israel Program for Scientific Translations, Jerusalem, 1965, 242 pp.)

Ghil, M., M. Halem, and R. Atlas, 1979: Time-continuous assimilation of remote-sounding data and its effect on weather forecasting. Mon. Wea. Rev., 107, 140-171.

Hoke, J. E., 1976: Initialization of models for numerical weather prediction by a dynamic initialization technique. Ph.D. Thesis, The Pennsylvania State Univ., University Park, Pa., 202 pp.

Fig. 1

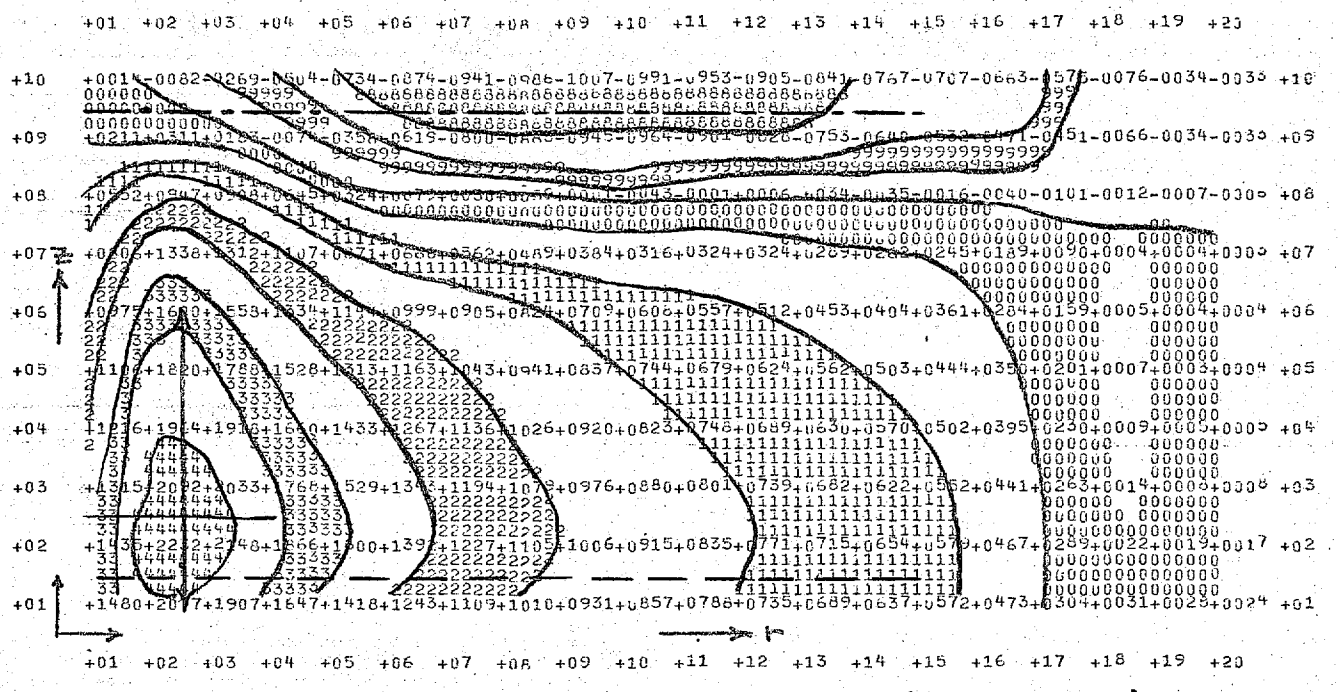

Tangential Wind Speed (m/sec x 100)
Case #54

1-level ASDL and range

1-level hi-frequency picture satellite cloud-tracked winds (low)

" (high)

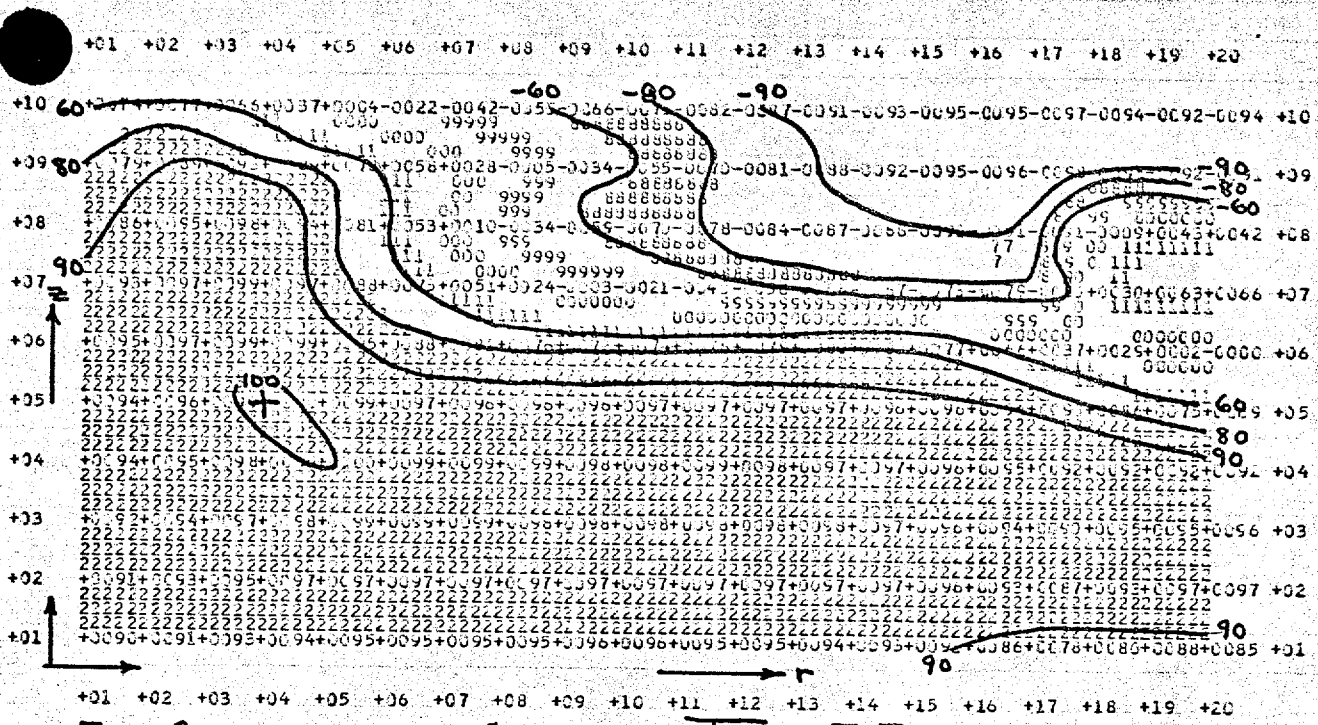

Fig. 2a Correlation $\overline{V_+' V_{r_2}'} / (\overline{V_+'^2}\,\overline{V_{r_2}'^2})^{1/2} \times 100$
Ensemble (82 cases)

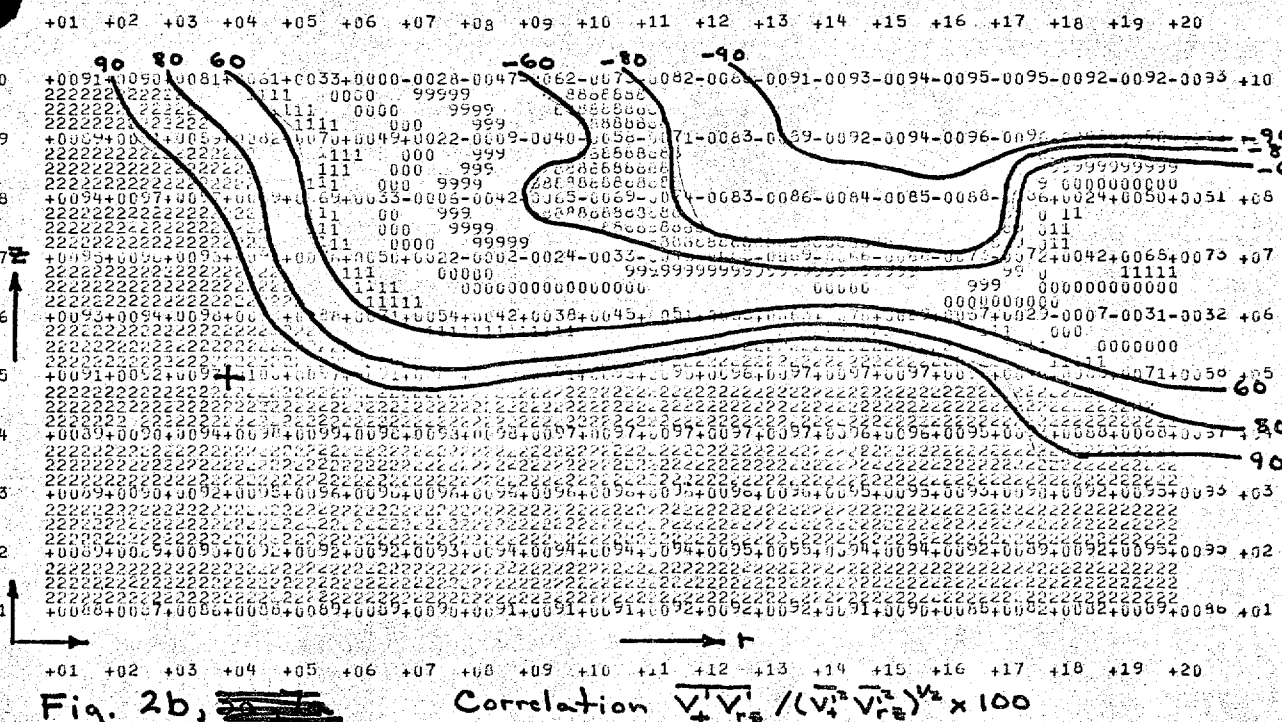

Fig. 2b, Correlation $\overline{V_+' V_{r_2}'} / (\overline{V_+'^2}\,\overline{V_{r_2}'^2})^{1/2} \times 100$
Subensemble #54

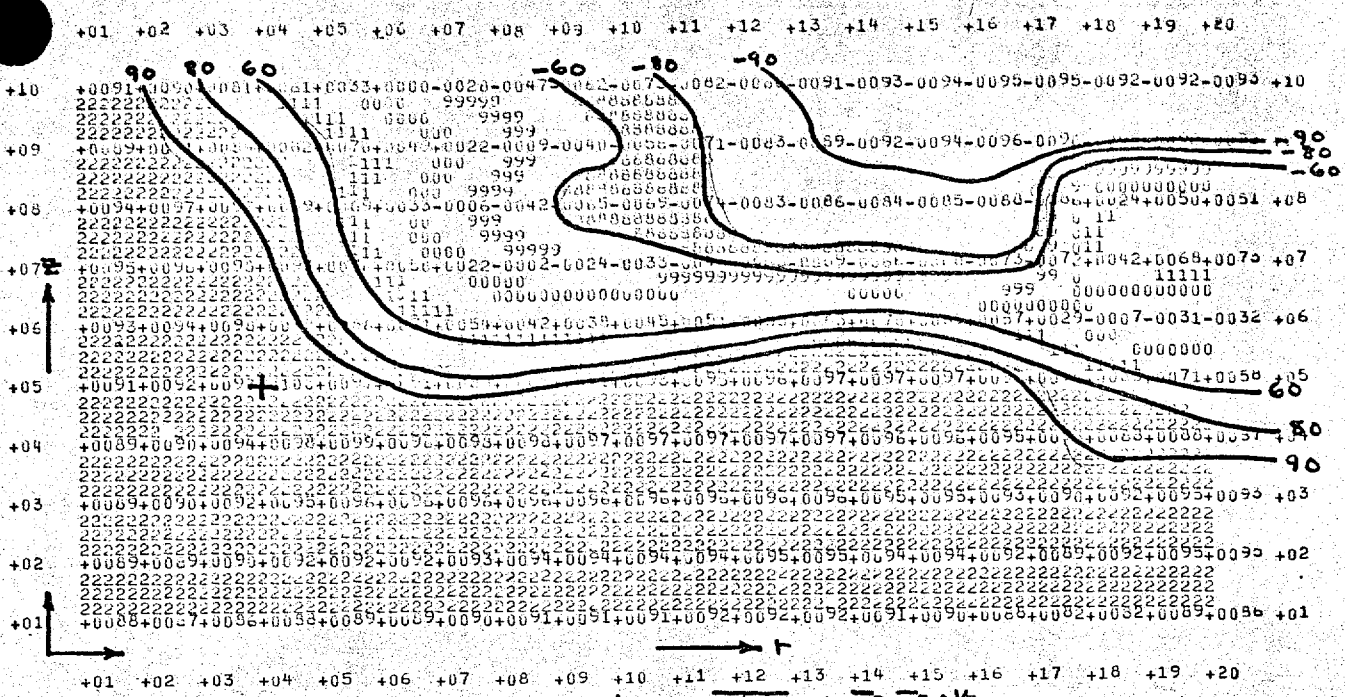

Fig. 3a Correlation $\overline{V_+' V_{r_2}'} / (\overline{V_+'^2}\,\overline{V_{r_2}'^2})^{1/2} \times 100$
Subensemble #54

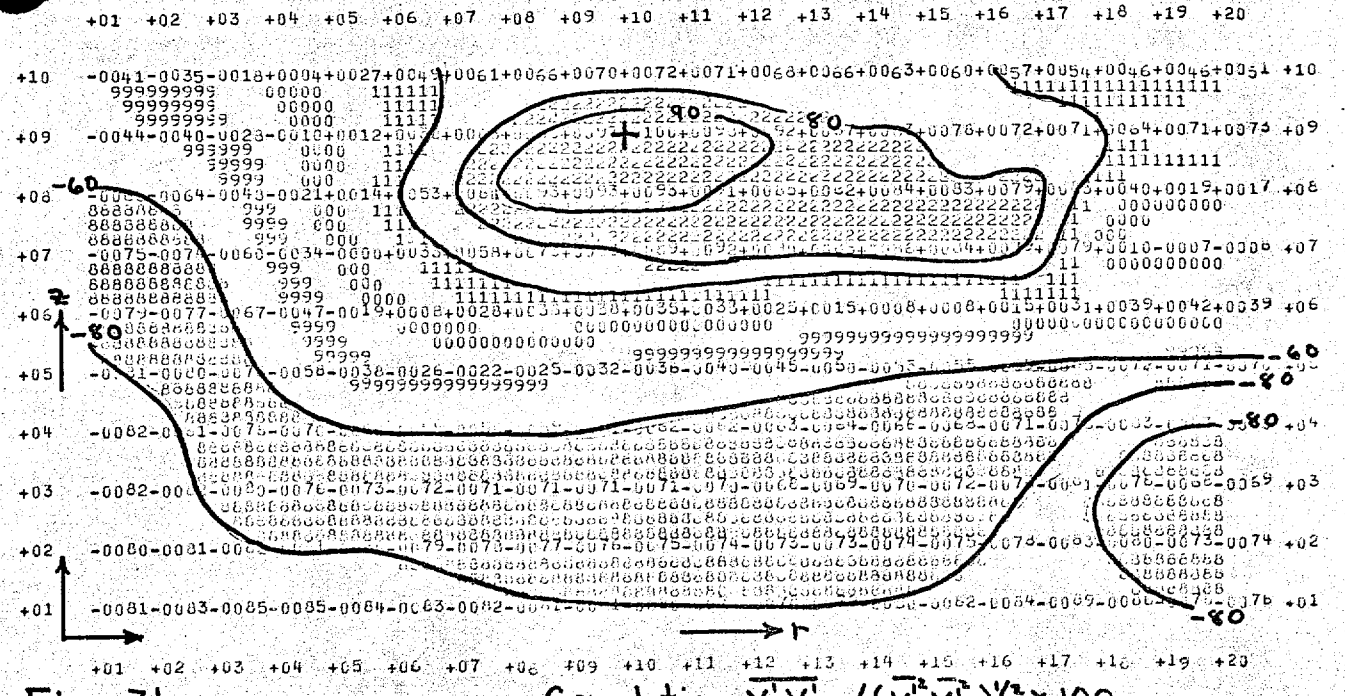

Fig. 3b Correlation $\overline{V_+' V_{r_2}'} / (\overline{V_+'^2}\,\overline{V_{r_2}'^2})^{1/2} \times 100$
Subensemble #54

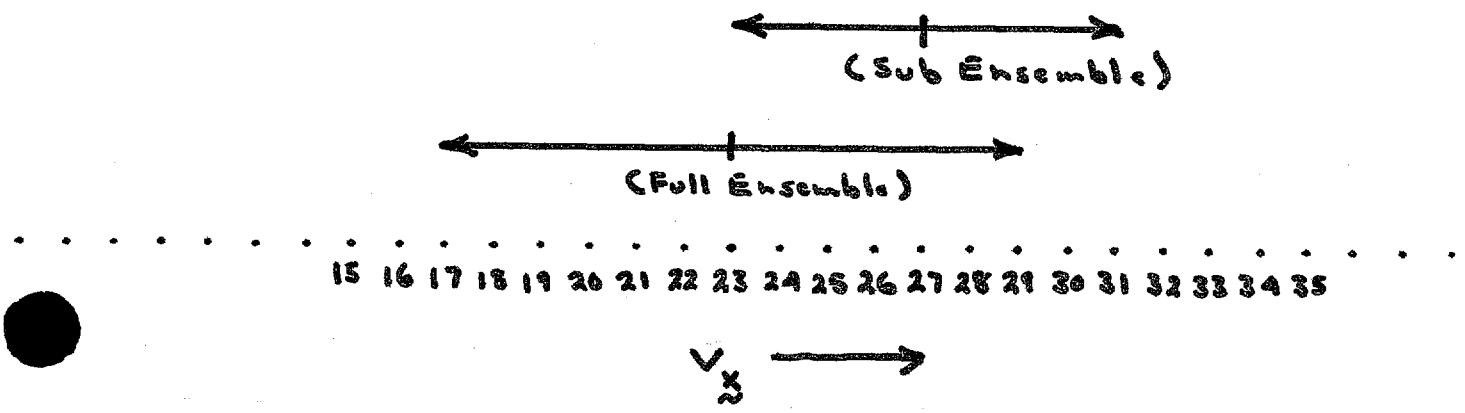

Fig. 4.
Schematic of mean and 2σ-limits of v at x for full- and sub-sample of cases.

Fig. 5a. Analysis of tangential wind with no data editing.
Contour interval, 5 m/sec.

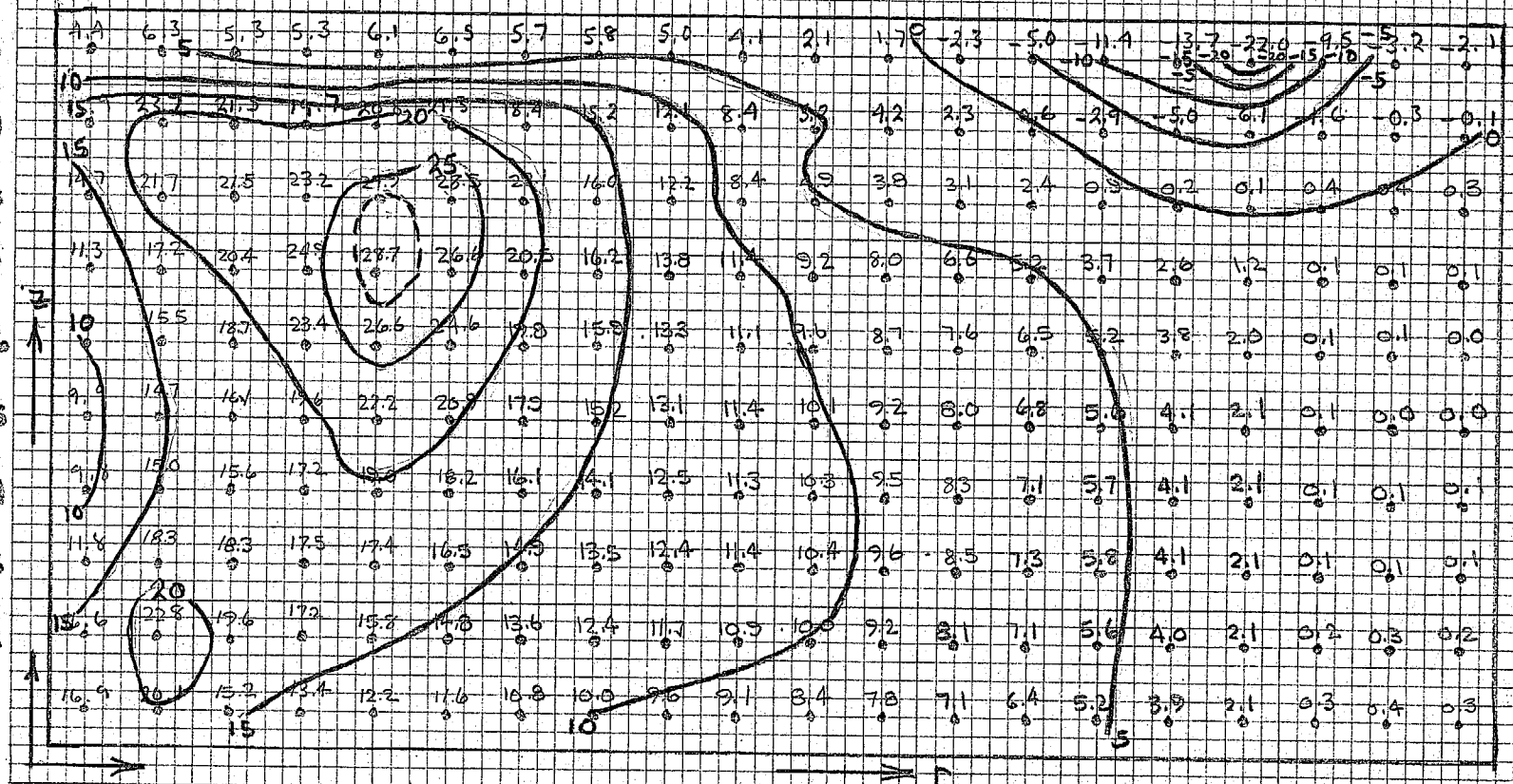

Fig. 5b. Analysis of tangential wind with data editing.
Contour interval, 5 m/sec.

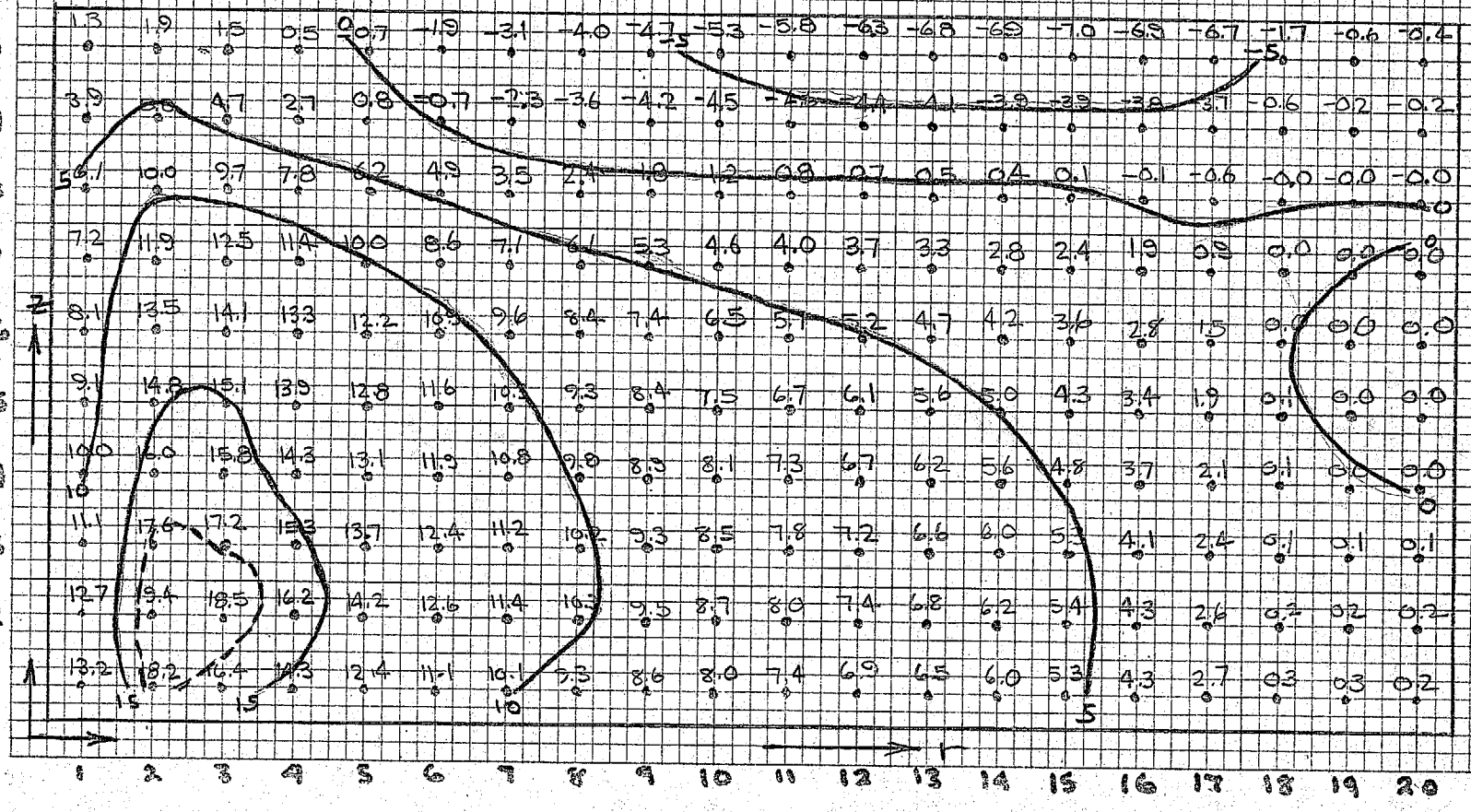

Fig. 6

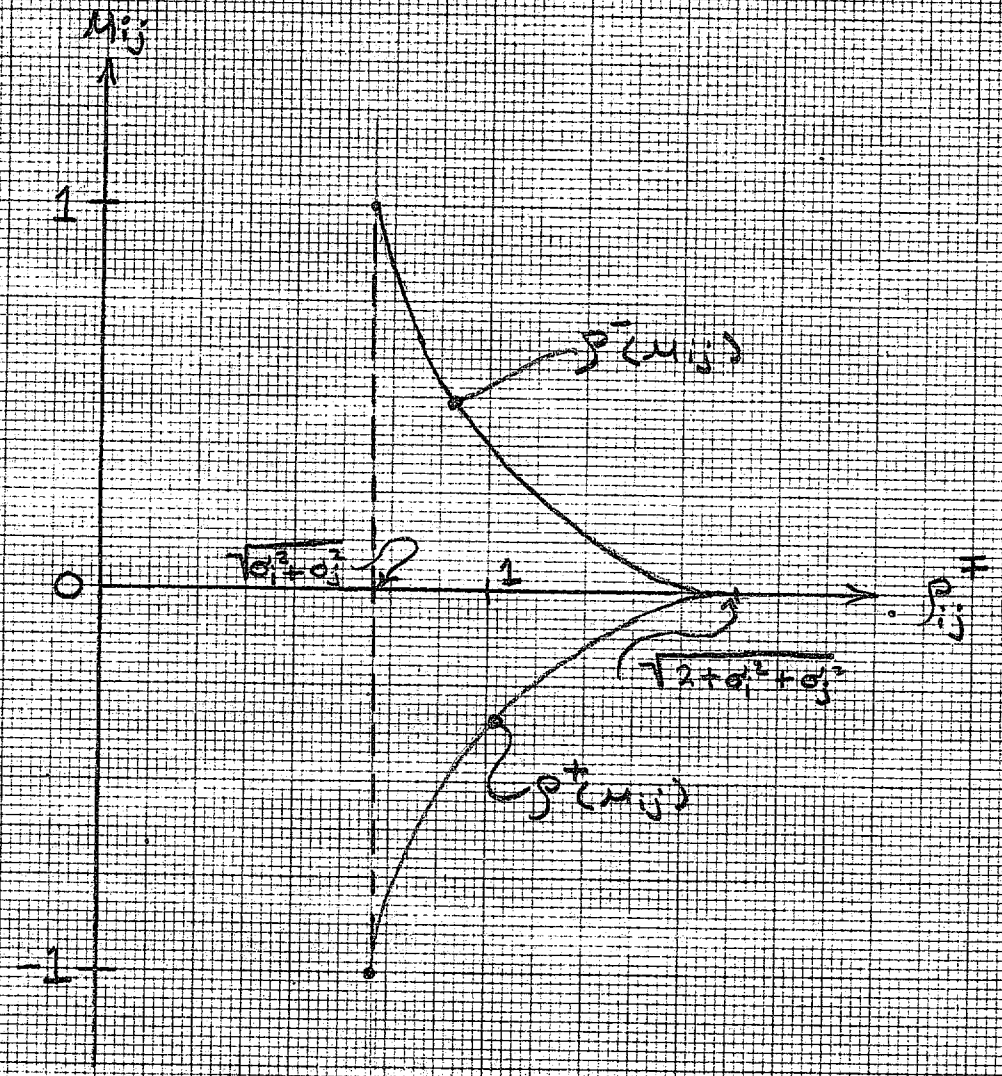

$$\rho_{ij}^{\mp} = \sqrt{2(1 \pm \mu_{ij}) + \sigma_i^2 + \sigma_j^2}$$

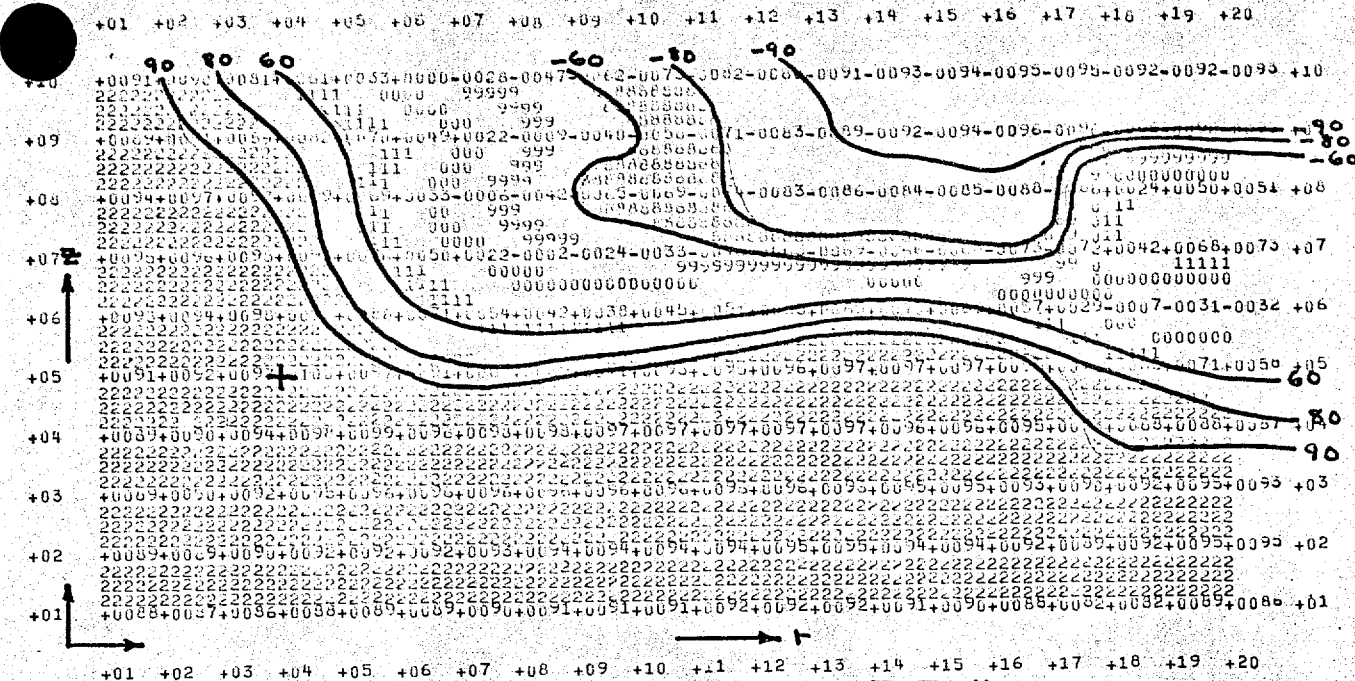

Fig. 7a Correlation $\overline{v_+' v_{r_2}'} / (\overline{v_+'^2}\,\overline{v_{r_2}'^2})^{1/2} \times 100$
Subensemble #54

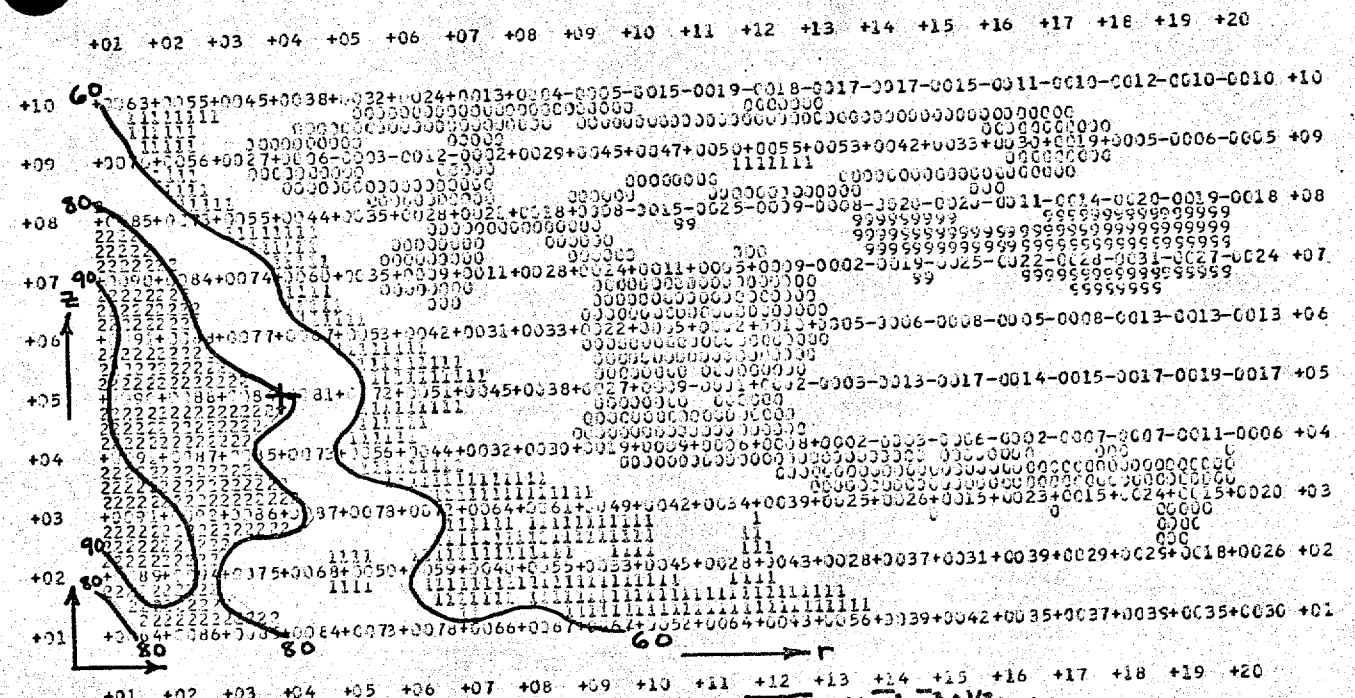

Fig. 7b Correlation $\overline{v_+' \theta_{r_2}'} / (\overline{v_+'^2}\,\overline{\theta_{r_2}'^2})^{1/2} \times 100$
Subensemble #54

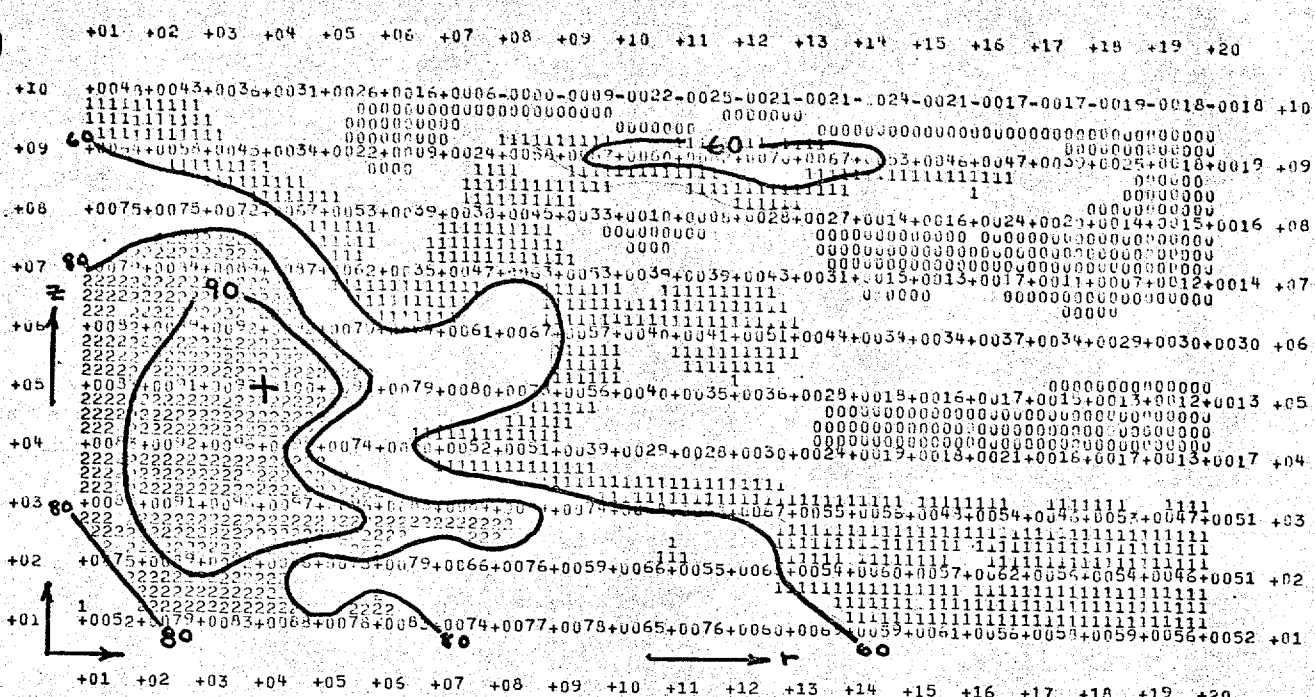

Fig. 8a Correlation $\overline{\theta'_+\theta'_{r_2}}/(\overline{\theta'^2_+}\,\overline{\theta'^2_{r_2}})^{1/2}\times 100$
Subensemble #54

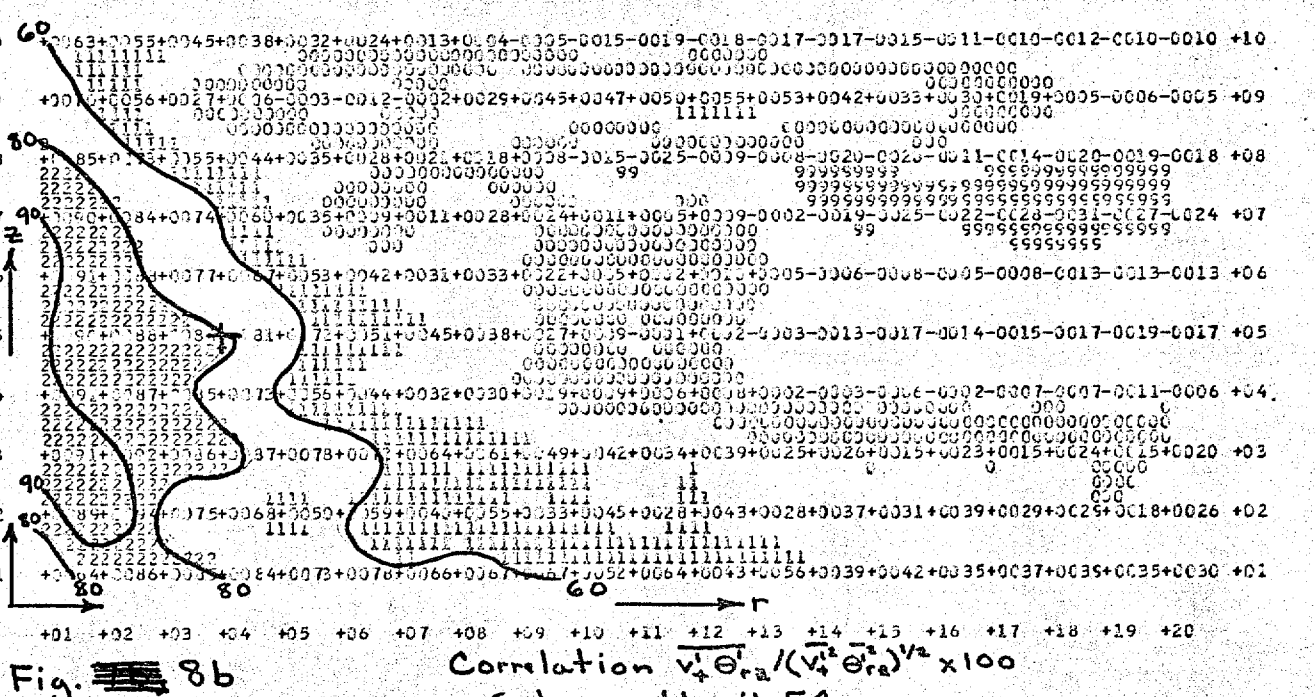

Fig. 8b Correlation $\overline{v'_+\theta'_{r_2}}/(\overline{v'^2_+}\,\overline{\theta'^2_{r_2}})^{1/2}\times 100$
Subensemble #54